PITS, SPOTS, UPLIFTS, AND SMALL CHAOS REGIONS ON EUROPA: EVIDENCE FOR DIAPIRIC UPWELLING FROM MORPHOLOGY AND MORPHOMETRY. Kelsi N. Singer[1], William B. McKinnon[1], and P.M. Schenk[2], [1]Department of Earth and Planetary Sciences and McDonnell Center for the Space Sciences, Washington University, St. Louis, MO 63130 (ksinger@levee.wustl.edu, mckinnon@wustl.edu), [2]Lunar and Planetary Institute, Houston, TX 77058 (schenk@lpi.usra.edu).

Introduction: Constraining the thickness of the ice shell on Europa and the geological processes occurring in it are key to understanding this icy world. We focus on features generally agreed to have been created by endogenic upwellings in the ice shell or ocean: pits, uplifts, spots, and subcircular chaos. We take advantage of topographic information for classification and as an aid to interpretation of possible formation mechanisms. Our data support a diapiric interpretation (as opposed to purely non-diapiric, melt-through models) and place lower limits on ice shell thickness at the time of feature formation, all conclusions testable by radar sounding on a future mission (such as EJSM).

Mapping Method: Our mapping was conducted over the two large, N-S mosaics taken during the Galileo mission's regional mapping campaign (East and West RegMaps). Feature sizes and topographic expressions were determined over the two areas richest in subcircular features: the northern section of the West RegMap and the southern section of the East RegMap, essentially completing the mapping first described in [1]. Resolutions of the base image mosaics are 220 and 210 m/px for the East and West maps, respectively. Features were identified based on morphology and further classified based on topography and albedo. Feature types were defined in a similar manner to [2,3], and definitions are given in [1]. All circular to subcircular features were mapped, including pits, uplifts, spots and chaos. We did not map all incidents of non-circular chaos, as previous studies have focused on such [2,4-8].

These features likely lie in a continuum of surface expressions from a similar mechanism of subsurface upwelling [8], but for the purposes of utilizing the topographic data they are defined as separate units. Topographic data were derived from albedo controlled photoclinometry (by PMS) and cross-checked with stereo data where possible. After the features were identified visually, topographic profiles were used to confirm and define their extent. The difference between the average elevation of the surrounding terrain and the minimum/maximum elevation of pits/uplifts was used to obtain feature depths /heights (results in Fig. 1, 4).

Results: Feature areas were measured and their size represented by the equivalent circular diameter. For the mapped portion of the East RegMap, the effective pit diameters are approximately log-normal distributed, with a peak (mode) near 4-5 km (Fig. 2). For the

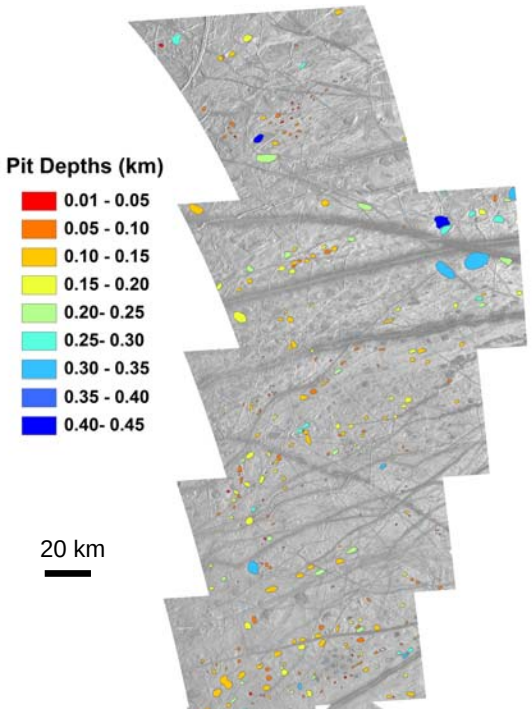

Figure 1. Pits color-coded by depth on the West RegMap which extends from 207° to 246° W longitude and from 62° N to 52° S latitude. Deeper pits (blue) are generally larger than shallow pits (red). Also see Fig. 5. Groupings of similarly sized and deep pits are apparent.

mapped portion of the West RegMap effective pit diameters more resemble a truncated normal distribution with a broad peak from ~2-6 km, although the ensemble of pits and small chaos could be log-normal distributed, with a peak near 5 km (Fig. 2). Uplift sizes have a peak around 6-7 km on the East map and between 3-5 km on the West map. The average pit depth is 120-140 km but they range from very shallow (~10 m) to ~ 500 m deep (Fig. 3). The average uplift height is from 90-130 km with a range from ~10 m to ~300 m.

We note that pit depths increase with increasing pit diameter (Fig. 1, 4). Although there is some spread to the data, this general trend is consistent throughout the range of pit sizes from 1 km to over 20 km. Additionally, larger uplifts have higher peak elevations. We also note geographic clustering (sometimes linear) of pits and small chaos features of similar character.

Discussion: This study finds a peak in the size distribution for all pits, and indeed for all features com-

bined, at ~4-5 km diameter, well above the effective resolution for ~circular feature identification (5 px ~ 1.1 km). Features smaller than 1-km diameter can be seen, such as small dark pit-like features 3-5 pixels across, but these appear to be part of larger chaotic disturbances in almost all cases. It cannot be ruled out that smaller features exist below the resolution limits in these areas, but what are mapped are features that can be verified with topography and are plausibly single expressions of upwelling. We have also examined those images with resolutions higher than the RegMaps. The areal coverage of these images is relatively small, but a preliminary survey does not show smaller and smaller pits.

The trend for greater diameter features to be deeper does not support the melt-through hypothesis for feature formation [9]. If water nearly melts through to the surface to form a pit, then the floor of the pits would likely reach a level of isostatic compensation based on the shell thickness, not an increasing depth with increasing pit size. The correlation of pit sizes and depths is more easily understood within the context of a diapir formation model. It is possible continued tidal heating could induce partial melting in an ascending diapir, and either the water could drain back into the ocean below, or if it occurs when the diapir is near the surface or the elastic lid of the ice shell, could form a water-rich lens [10]. This loss of volume could lead to isostatic compensation in the form of a pit. The larger the diameter of the diapir the more volume is available for potential melting and volume loss, resulting in a deeper pit.

Regardless of formation mechanism, we can estimate a lower limit for shell thickness using a simple isostasy model. In a theoretical endmember case where the column of material below a pit has been replaced by liquid except for an arbitrarily thin lid, the shell thickness is given by $\rho_l d/\Delta\rho$, where ρ_l is the density of the liquid, d is pit depth, and $\Delta\rho$ is the density contrast between the shell and the liquid. Different compositions can be envisioned [11], but a plausible range of $\Delta\rho$ and conservative maximum pit depths of ~450 m imply a *minimum* shell thickness on Europa of ~4-to-9 km.

Conclusions: A peak in the size-frequency distribution for all feature types is seen at ~4-5 km in diameter. Topographic data reveals that most pits are ~100 m deep, but a few are as deep as ~500 m. This range of pit depths fits numerical simulations by [12,13], but observed pit sizes are smaller and the morphologies differ. Larger pits are consistently deeper than smaller ones, a result that does not match a feature formation due to melt-through to the surface. A conservative estimate based on some of the deepest pits suggests a *minimum* shell thickness of ~4-9 km if they formed in isostatic balance. Such an estimate may appear to favor a thicker ice shell, as indeed any evidence for diapirism does, but Europa is a dynamically evolving [14] and likely thermally evolving world [15]. Substantial ice shell thickness variations over time are plausible, and our conclusions regarding formation mechanism and shell thickness strictly refer to the epoch of feature formation, conclusions which are testable (e.g., by radar sounding) on a future mission such as EJSM.

References: [1] Singer K.N. et al. (2009) *LPSC XL*, abs. #2336. [2] Spaun N.A. (2002) Ph.D Thesis, Brown Univ. [3] Spaun N.A. et al. (2004) *LPSC XXXV*, abs. #1409. [4] Greenberg R. et al. (1999) *Icarus 141*, 263286. [5] Greeley R. et al. (2000) *JGR 105*, 22,55922,578. [6] Riley J. et al. (2000) *JGR 105*, 22,559–22,578. [7] Figueredo P.H. and Greeley R. (2004) *Icarus* 167, 287-312. [8] Collins G. and Nimmo F. (2009) in *Europa*, UA Press, 259-282. [9] Greenberg R. et al. (2003) *Icarus 161*, 102–126. [10] Sotin C. et al., (2002) *GRL* 29, 74-1. [11] McKinnon W.B. and Zolensky M.E. (2003) *Astrobiology 3*, 879-897. [12] Han L. and Showman A.P. (2005) *GRL* L20201. [13] Showman A.P. and L. Han (2005) *Icarus 177*, 425-437. [14] Lainey. V. et al. (2009) *Nature 459*, 957-959. [15] McKinnon W.B. et al. (2009) in *Europa*, UA Press, 697-710.

Figure 2

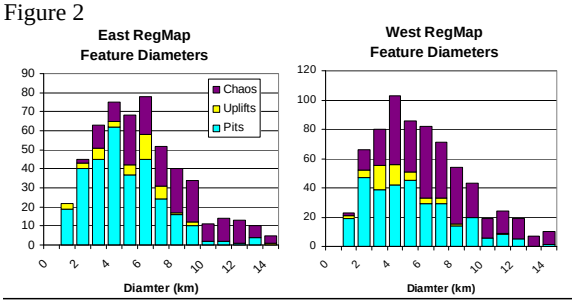

Figure 3

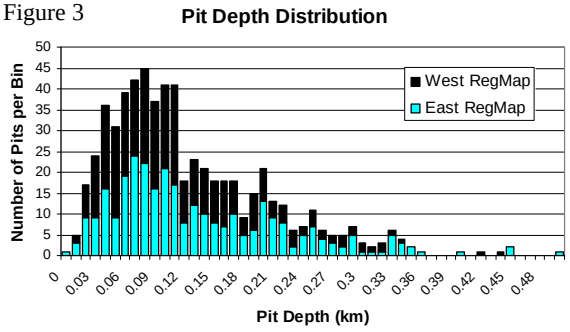

Figure 4

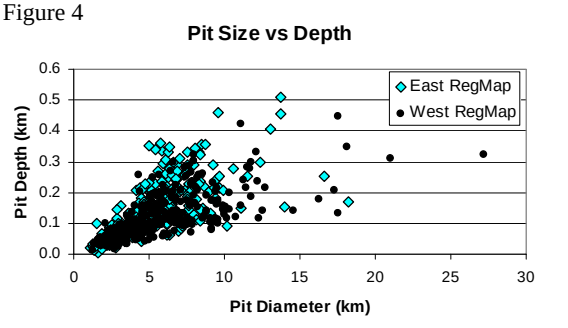

Figures 2-4. Morphometric data for pits, uplift, and small circular to sub-circular chaos features on Europa. Note that an extended tail of features exist between 15-30 km effective diameter (not shown in Fig. 2; cf. Fig. 4).